Journal of Electromagnetic Waves and Applications, 2014
Vol. 28, No. 1, 1–12, http://dx.doi.org/10.1080/09205071.2013.850454

Taylor & Francis
Taylor & Francis Group

A linear array quasi-lumped element resonator antenna with a corporate-feed network

S.S. Olokede* and M.F. Ain

School of Electrical and Electronic Engineering, Universiti Sains Malaysia, Nibong Tebal, Penang 14300, Malaysia

(*Received 3 May 2013; accepted 19 September 2013*)

A linear array quasi-lumped element resonator antenna with parallel feed network is presented. The proposed antenna was excited by a corporate feed network. The antenna element consists of the interdigital capacitor in parallel with a straight narrow strip inductor. The inductor is the centre finger and shorted across the interdigital capacitor. With the pads connected at both ends of the structure, adjustment to tune the resonant frequency of the resonator is possible. Seeing that the proposed antenna is a lumped element, it is estimated that significant size reduction is realizable with attendant low mass, low volume, and low cost. Therefore, the individual radiating element has a small footprint area of $0.112\lambda_0 \times 0.108\lambda_0$, and thus reduced the overall antenna real estate moderately. The measured gain of the array operating at 5.8 GHz is 16.20 dBi. The proposed antenna exhibits moderate bandwidth enhancement and reasonable directional characteristics.

Keywords: antenna size; corporate network; interdigital; quasi-lumped element; series array

1. Introduction

Existing design methods that have been employed to feed printed microwave antenna arrays can be categorized into series and parallel feeds.[1] In general, the series feed configuration is a more compact network as it requires less transmission lengths, fewer junctions and lower insertion loss. It however suffers from narrow bandwidth, and inherent phase difference caused by the differences in the lengths of feed lines.[2] Alternatively, the corporate fed configuration has a relatively wide bandwidth since it does not suffer from high mismatch losses.[3] Much more, the advantages of corporate or parallel feeds as excitation networks for printed antenna arrays have great design flexibility and ease of vertical integration to form a two-dimensional array.[4] It allows easy control of the feed of each of the element (both in terms of magnitude using amplifiers/attenuators, and phase using phase shifters), and as such, ideal for scanning phased arrays, multibeam, or shaped-beam arrays. Equal excitations can also be achieved, but at the expense of compactness.

Radiation from the feed line is a serious problem that degrades the cross-polarization and side lobe levels of the arrays.[5] In addition, the antenna element copper losses, feed resistive and radiation losses obviously lead to gain and radiation pattern limitations. Losses in the patches and microstrip corporate feeds are largely due to cop-

*Corresponding author. Emails: solokede@gmail.com, sso10_eee044@student.usm.my

per and dielectric losses in straight lengths compounded with radiation and surface-wave losses from the overall structure, the complete quantification of that requires detailed knowledge of the current distribution on the antenna elements and the feed network. In [6], just as in [7], it was identified that mutual coupling between elements can introduce scan blindness, and hence a limitation, which is strongly influenced by the presence of surface waves. While, it is a possibility in circular polarization for the cross-polarization and side-lobe levels to be improved by isolating the feed network from the radiating surface, it is however not the focus of this study. The use of photonic band gap [8] or cavities in conjunction with microstrip element [7] will undoubtedly minimize surface-wave losses. Instead, we intend to explore, amongst others, the feasibility of optimizing these losses to the intent of achieving better performance, and secondly, capitalize on the reduced capacity of the proposed resonator to realize a compact corporate-fed antenna, yet with good efficiency.

To this end, a single quasi-lumped element resonator antenna is introduced in order to achieve compact size vis-à-vis its operational performance. The belief is that, if the single element is small, there is a likely possibility that the array may also be small. Thereafter, design of a linear array quasi-lumped element resonator antenna with corporate feed network will be implemented, with a view to obtain an array configuration structure with a reduced antenna real estate. The earlier identified losses will be assessed, and optimized for performance enhancement. It is estimated that the size of a single radiating quasi-lumped element is 5.8 mm × 5.6 mm, and thus expectedly, will reduce the antenna real estate to an extent. Besides, quasi-lumped elements have proved themselves to be ideal candidates for antenna applications by offering several advantages including mechanical simplicity, large impedance bandwidth, simple coupling schemes to all commonly used transmission line, very high radiation efficiency, can be made smaller than conventional metal antennas and low cost. They are therefore suitable for monolithic MICs and for broadband hybrid MICs where small size requirements are of prime importance.[9] The resulting design is simple, easy to fabricate and show a reasonable bandwidth and directional characteristics.

2. Theoretical framework

2.1. The proposed resonator

Lumped element is by definition much smaller than their wavelength. Therefore, microstrip line short and stubs, whose physical lengths are smaller than a quarter wavelength λ_g at which they operate, are the most common components for approximate microwave realization of lumped elements in microstrip resonator structures, and are termed quasi-lumped elements.[6] The part of the resonator where the magnetic energy is stored is separated from the part where electric energy is stored. The advantage of this approach is the direct transformation of an equivalent circuit consisting of capacitors and inductors into a microstrip structure. It has a capacity to admit the highest Q-factor, due to minimal surface resistance. At microwave frequencies, a microstrip quasi-lumped element is a reasonable resonator in terms of smaller footprint and Q-factor of about 8000. However, the high Q-factor restricts the bandwidth, which limits its usefulness as an antenna.[9–16] Figure 1 shows the proposed single element quasi-lumped resonator and equations to find the resonant frequency for the proposed antenna are given in Ref. [17].

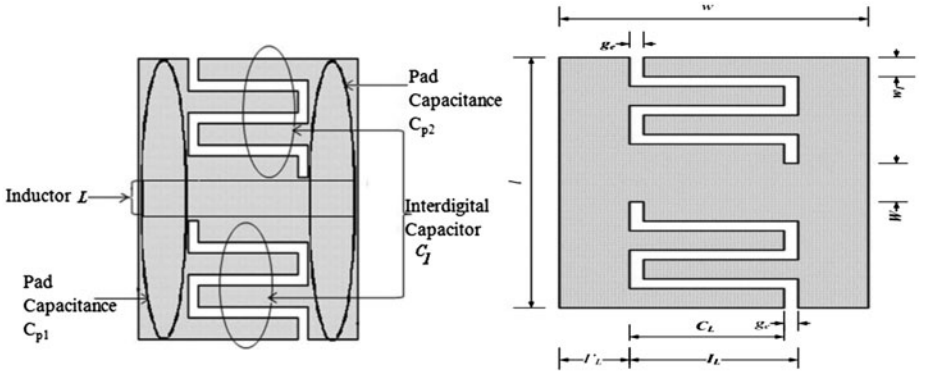

Figure 1. A single quasi-lumped element resonator.

2.2. *The corporate feed*

There are four broad classes of losses in corporate network. The first one is conductor losses otherwise known as the ohmic losses, the radiation losses, surface-wave losses and lastly, the dielectric losses. While, the dielectric losses are the losses in the substrate, the losses in the transmission line is the ohmic losses, the losses due to surface waves is surface-wave losses and finally, radiation energy losses which are due to the conversion of radiation energy to heat energy.

Consider the microstrip line sections in Figure 2 with eight-element quasi-lumped resonator as the load on one end of the transmission lines and matched source at the other end. The source current at the input terminal is

$$I = I_0 e^{\mathrm{j}wt} \tag{1}$$

Therefore, the current in a transmission line which is fed at its end by the voltage $V_0 e^{\mathrm{j}\omega t}$ and loaded by the radiating elements of resistance R at its other side is reported in Ref. [18], where $I_0 = V_0/Z_c, \beta = k_0\sqrt{\varepsilon_{\mathrm{eff}}}$ is the constant of propagation in the transmission line, W is the width of the line and Γ is the reflection coefficient at the load end of the line. In order to calculate the radiation loss from this microstrip lines, Levine et al. in [19] presented a rigorous analysis of the radiation and the losses of microstrip arrays including the feed network. In their work, the closed equations to determine

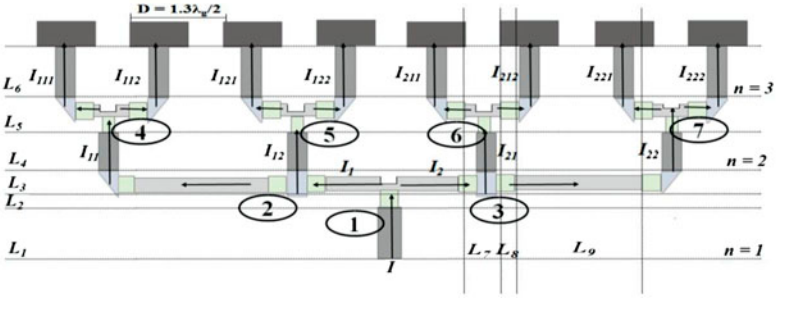

Figure 2. The current distribution in the microstrip lines of the proposed antenna.

radiation loss as well as the surface-wave loss as a function of input power and characteristic impedances were reported. It was identified in [18] that the real part of the complex input power in microstrip transmission lines dissipates first by propagation of surface waves in the visible range, the region defined by the condition $k_x^2 + k_y^2 \succ k_0^2$ and lastly, by radiation loss into space which occur within the visible range by a condition $k_x^2 + k_y^2 \prec k_0^2$. The exact formula to determine the radiation losses at the discontinuities as well as its form factor were reported by Lewis [20,21] and they are as stated. In [21,22], equation to determine the form factor was reported, where $F(\varepsilon_{\text{eff}})$ is the form factor. It was reported in [19] that the input power converted into surface waves varies directly with $(h\sqrt{\varepsilon_r}/\lambda_0)^3$, whereas the percentage radiated into free space varies as $(h\sqrt{\varepsilon_r}/\lambda_0)^2$, for every small h/λ, where h is the substrate thickness. Under this assumption, it will be expedient to keep $h\sqrt{\varepsilon_r}/\lambda_0$ low, in order to reduce the radiation loss. It is noteworthy, therefore, that the percentage of power converted into surface waves is negligible when compared with considerable amount of power radiated into space. Besides, percentage power converted into surface waves does not, to a significant extent affect the characteristics of the portion radiated into space under assumption of infinitely large substrate. Hence, part of our work is to first substantiate this assumption by calculating the actual value for the proposed feed, and then focus on the radiated power, around the vicinity of the real part of the complex power that appears in the visible range as defined earlier. This is because the radiation loss of a microstrip transmission line with a given thickness and characteristic impedance depends on the line length, and also, oscillatory in nature. Hence, the losses grow with $(L/\lambda_0)^2$ in the range $0 < L > \lambda_0$, and insensitive otherwise. Knowing that losses are proportional to $1/Z_C$, both the radiation power (P_r) and surface-wave excitation (P_S) are loosely dependent on Z_C. However, the ohmic and dielectric losses are significant particularly in the dominant microstrip mode. Henceforth, equations to determine the dielectric and ohmic losses in dB/cm are reported in [23–25], where q is the dielectric filling factor already defined by Wheeler [26] as the ratio of stored electric field energy to the total feed energy in a microstrip, but the closed-form equation was stated by Schnieder [27], α_d is the dielectric attenuation factor, α_o is the ohmic attenuation factor, $\tan\delta$ is the loss tangent and p is the magnetic power factor. The power radiated into surface waves has a different dependence on h/λ for small values, as compared to free space radiation. Therefore, power radiated into surface waves is stated in [22]. Finally, it was demonstrated by Lee and Hayakawa [28,29] that a right-angle bend with one corner (analogous to each of the two extreme bends on line L_3 in Figure 2) exhibit larger radiation loss than that of a straight line by about 2–8%, but smaller than that of similar bend with many corners, T-junction (analogous to junctions 2–7, also in Figure 2) by 2–7% for perfect conductor and otherwise for an imperfect conductor. However, the right-angle bend have high voltage standing wave ratio (VSWR) due to increased inductance. Therefore, decrease in input reflection coefficient can be achieved if the corner is chamfered (mitered) via an instrumentality of increased inductance or decreased capacitance techniques.

3. Antenna design

3.1. *Quasi-lumped element resonator*

The proposed resonator design was reported in [17] and depicted in Figure 1(b) earlier. The length (l) of each of the radiating element was 0.58 cm, whereas its breadth (w) was 0.56 cm, with $N = 8$, where N is the number of interdigital fingers. The width of

each finger (w_1) was 0.035 cm, a length (C_L) of 0.305 cm and inter-finger width (g_e) of 0.03 cm. The width of the centre finger, otherwise known as the narrow strip inductor (W), was 0.12 cm which is of the same length with the interdigit fingers. The pad width (I'_L) was calculated to be 0.1125 cm.

3.2. *Design of corporate feed network*

3.2.1. *The Feed Design*

Figure 3 shows the design parameter in terms of widths of the proposed corporate feed array while Figure 2 shows their respective line lengths. In Figure 4, fabricated prototype of the proposed antenna was depicted. The width (w_1) was 0.1898 cm approximately equal to 50 Ω, w_2 is equal to 0.105 cm (70.7 Ω), w_3 was 0.046 cm (100 Ω) and finally, w_4 = 0.6, w_3 = 0.03 cm (though the values was supposed to be 0.028 cm because of etch limitations). All the widths were determined using Equations (7) and (8) listed in [29] for different values of Z_C. The length L_1 was 0.4 cm, L_2 (= L_8) was $\lambda/4$ (= 0.7 cm), L_3 was 0.1898 cm, L_4 was 0.6 cm (which was equal to L_6), $L_5 = L_2 + L_3$ (= 0.8898 cm), L_7 was 0.315 cm and L_9 was 1.925 cm. The total length L_T (in y-direction) was 3.3 cm, while the total length (in x-direction) was 13 cm (0.58 + 7(1.82)). Therefore, the antenna size was about 3.3 cm × 13 cm.

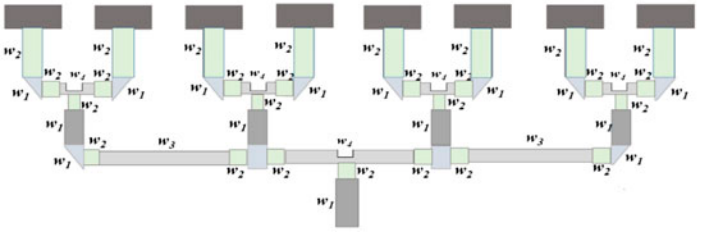

Figure 3. The design parameters of the proposed antenna.

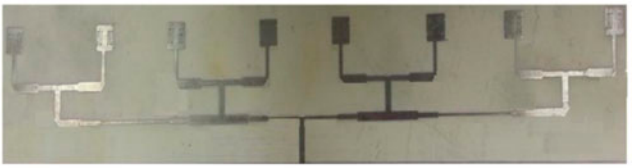

Figure 4. The fabricated prototype of the of the proposed antenna.

Table 1. Design parameters for optimization.

S/N	w (mm)	w/h	10 h/w	q	p	ε_{eff}	$\varepsilon_r/\varepsilon_{eff}$	$q(\varepsilon_r/\varepsilon_{eff})$	$F(\varepsilon_{eff})$	$\alpha_d \times 10^{-3}$ (dB/mm)	α_o (dB/mm)
1.	1.898	2.33	4.28	0.719	0.8	2.710	0.802	0.576	2.170	1.517	0.780
2.	1.05	1.29	7.74	0.669	0.98	2.592	0.767	0.513	2.198	1.350	0.956
3.	0.46	0.57	17.67	0.616	1.12	2.465	0.729	0.449	2.230	1.182	1.092
4.	0.3	0.37	27.10	0.595	1.31	2.415	0.714	0.425	2.243	1.112	1.277

3.2.2. The Design Optimization

3.2.2.1. Dielectric loss (P_d)

Considering Figure 2, the overall dielectric losses were calculated by multiplying dielectric attenuation factor (α_d) with their respective lengths of the line. From Tables 1 and 2, therefore, the dielectric loss as a result of length L_1 is 0.0601 dB, L_2 is 0.0142. Similarly, the dielectric loss in L_3 is 0.617, L_4 is 0.144, L_5 was equal to 0.480 dB, L_6 was 0.648, L_7 was 0.064, L_8 was 1.323 and L_9 was 0.683. Hence, the total loss on the line was 0.004 dB. Thus, it was observed that the dielectric attenuation loss factor shown in Table 1 differs not much irrespective of their width. To that extent, dielectric loss does not depend on the transmission line geometry, but rather on the loss tangent (tan δ) of the substrate material. Therefore, a substrate of loss tangent of 0.0027 was used to reduce the loss.

3.2.2.2. Ohmic loss (P_O)

The same procedure applicable to calculate the dielectric loss was repeated to determine the ohmic losses. The ohmic loss for each line was documented in Table 2. Hence, the total ohmic loss across the lines was 2.858 dB. It was noted that the ohmic attenuation factor, and by extension, the ohmic loss increases with narrow line width and higher impedance. Take for instance in Table 1, the ohmic loss coefficient for a width of 0.1898 cm (Z_C = 50 Ω) was 0.780, while that of 0.03 cm (Z = 105 Ω) was 1.277. It was also noticed particularly in Table 1, that the loss was proportional to the skin resistance of the metal and thus goes up with square root of frequency. To reduce the loss, a metal thickness (t) of three times the skin depth was chosen which is equal to 0.0035 cm.

3.2.2.3. Radiation loss (P_r)

Radiation loss was not uncommon in transmission lines particularly at discontinuities either as open circuits, short circuits or corners. The radiated powers at these discontinuities were calculated. It was noted that the two largest contributors to radiation loss among various circuit discontinuities are junctions and the right-angle bends. Therefore, the strip corners were metred sufficiently to secure a large bend in order to satisfy a

Table 2. Loss computation due to optimization.

Line no.	w (cm)	No. of lines	Line lengths (cm)	$\alpha_d \times 10^{-3}$ (dB/cm)	α_o (dB/cm)	$P_d \times 10^{-3}$ (dB)	P_O (dB)	$P_r \times 10^{-6}$ (dB)	$P_s \times 10^{-9}$ (dB)
1.	0.1898	1	0.4	0.1517	0.0780	0.060	0.0312	3.34	0.495
2.	0.1050	1	0.7	0.1350	0.0956	0.014	0.0609	5.85	0.866
3.	0.1898	2	0.6	0.1517	0.0780	0.182	0.0936	10.00	1.485
		10	0.3	0.1517	0.0780	0.435	0.2340	25.06	3.712
4.	0.1898	4	0.1898	0.1517	0.0780	0.144	0.0592	6.34	0.939
5.	0.1050	4	0.8898	0.1350	0.0956	0.480	0.3400	29.73	4.404
6.	0.1050	8	0.6	0.1350	0.0956	0.648	0.4590	40.09	5.939
7.	0.0460	4	0.135	0.1182	0.1009	0.0640	0.0540	4.51	0.682
8.	0.1050	14	0.7	0.1350	0.0956	1.323	0.9370	81.85	12.126
9.	0.0460	3	1.925	0.1182	0.1009	0.683	0.5830	1.15	7.146
						4.033	2.8580	207.92	37.794
Total losses = 2.8622									

scenario whereby both the strip conductor thickness (t) and the grounded plane are assumed to be at least three to four skin depths thick. Also, radiation loss increases with $(h\sqrt{\varepsilon_r}/\lambda_0)^2$. Hence, a thin duroid RO4003C microwave substrate of dielectric permittivity of 3.38, a thickness of 0.0813 cm and a loss tangent ($\tan\delta$) of 0.00027 at λ_0 equals 5.172 cm was used. Doing this effectively reduces radiation loss to a large extent. In turn, it is expected that the reflection coefficient at the load end of the line decreases majorly and so is the return loss. It implies that the lower the reflection coefficient, the lower the radiation loss. Hence, a good matching condition is required to minimize radiation loss. To that extent, both the Wilkinson power divider and a quarter wavelength transmission line transformer were used for the matching condition.

3.2.2.4. Surface-wave loss (P_S)

The desire to minimize surface-wave losses suggest that high characteristic impedance be employed seeing surface-wave excitation is loosely dependent on the characteristic impedance Z_C. By implication, $1/Z_C$ will be sufficiently small to minimize surface excitation and hence its loss. Therefore, high impedances of 100 and 70.7 Ω were used through the instrumentality of Wilkinson power divider mechanism and the quarter wavelength transmission line transformer. A thin dielectric substrate was also used in the design to further reduce the surface-wave loss.

3.3. Design of the antenna array

The proposed antenna was prototyped using Finite Integration Technique solver, CST microwave office studio. The resulting design was fabricated on a Duroid RO4003C microwave substrate of permittivity of 3.38, a thickness of 0.0813 cm and metal thickness of 0.0035 cm, using a simple photolithographic technique. The fabricated design was excited with an optimized corporate feed network as shown in Section 3.2. As shown in Figure 2, the spacing between the array elements which depend on the guided wavelength was determined and consequently, each element was positioned at $1.3\lambda_g/2$ inter-element interval. This spacing is sufficiently long enough to overcome the mutual coupling effect between any two junctions. The choice of this value is principally to accommodate the corporate feed arrangement which would have been otherwise impossible using inter-element spacing of $\lambda_g/2$, even though it is logical to do so to minimize the side lobe level.

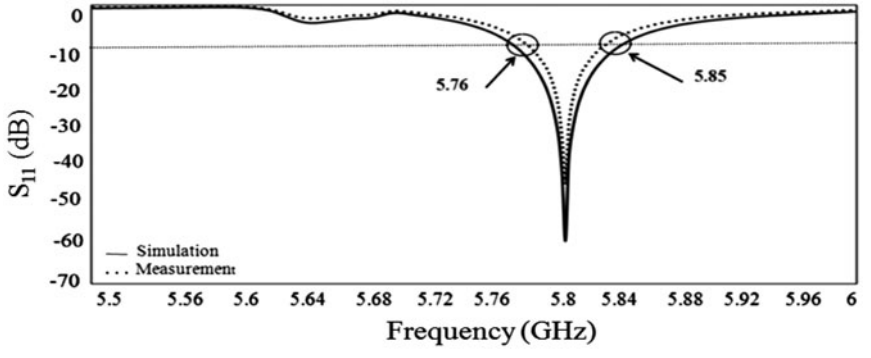

Figure 5. Simulated and measured return loss of the proposed antenna.

4. Result and discussion

Figure 5 illustrates the simulated and measured return loss of the proposed antenna. The simulated return loss was 60.09 dB, whereas the measured return loss was 50.01 dB with their respective simulated and measured frequency pattern of 5.77–5.87 and 5.76–5.85 GHz and at a resonant frequency of 5.8 GHz. The marginal impedance bandwidth was due to high *Q*-factor characteristic of the proposed antenna. Usually, quasi-lumped element resonator inherently exhibit high *Q*-factor and are often higher than that of overlay capacitors which are mostly larger in size. The *Q*-factor becomes more pronounced when high conductivity conductors and low-loss tangent dielectric substrate are used.[10] Much more pronounced is this effect when high temperature superconducting films are used.[30] As a result of this, the spacing between the resonator and the ground plane (in particular due to thin substrate used in this work) becomes smaller, and the resonator moved closer to the ground plate. To this effect, less energy is radiated and more energy is stored in the interdigit capacitor and the strip-centred inductor. The effect of this action strongly influenced the impedance bandwidth of the proposed antenna, and as such, responsible for the narrow bandwidth characteristics exhibited by the antenna. However, it was noted that using a coaxial feed probe could dampen the excessive resonance to a large extent, and hence improve the bandwidth to a degree that depends on both the height and aperture of the probe.

Though the discrepancies in the value of the simulated and measured return loss results were significant, their respective return loss results are far better that the moderate value of −10 dB with simulated and measured VSWR of 1.002 and 1.006, respectively. The VSWR which is a measure of how well a transmission line is matched to the load shows a perfect match. By implication, therefore, both the radiation and surface-wave losses have been significantly minimized. In general, the simulated and measured return loss plots show good agreement. The slim frequency pattern differential between the simulated and measured results further corroborated the efficiency of the feed.

Figure 6 shows the simulated and measured radiation pattern orientation of the proposed antenna in *xz*- and *yz*-planes. In both planes, co-polarization component was larger than the cross-polarization. This pattern indicates right-hand circular polarization

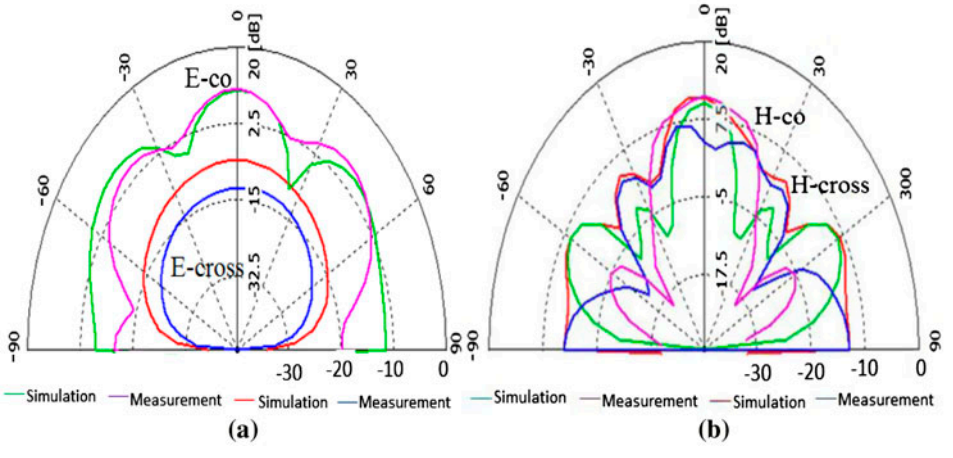

Figure 6. Simulated and measure radiation patterns, (a) *xz*-plane, (b) *yz*-plane.

tendency of the proposed antenna. In *xz*-plane, both simulated and measured co-polarization component was 25 dB larger than cross-component. The same scenario repeats itself in *yz*-plane, but with moderate value particularly against the measured cross-polarization component. In general, the main lobe magnitude was 10 dB oriented in 0° direction with beamwidth (HPBW) of Ω_{xz} = 22.2° and a side lobe level of −7.1 dB in *xz*-plane. In *yz*-plane, the main lobe magnitude was the same with *xz*-plane main lobe, oriented similarly, but with HPBW of Ω_{yz} = 17° and a side lobe level of −7.3 dB. In Figure 7, the normalized radiation pattern in Cartesian coordinate was presented. The measured 3-dB angular bandwidth of the main lobe was not too different from that of Figure 6. It is interesting to note that the beam width is narrower than that of a single element (who is known to be relatively wider) due to smaller 3-dB angular value. As a result of this, the radiation intensity of the proposed antenna is concentrated in the principal axis in a desired direction by converging the radiation pattern. This effect, in essence, is a measure of the directivity of the antenna. Consequently, the main lobe becomes more penetrating and suitable for long-range communications. Because of the minimized characteristic of HPBW, the gain of the antenna becomes reasonable, and hence sufficient for long-distance communications.

Figure 8 depicts the simulated and measured gain of the proposed antenna using gain absolute method. The simulated gain was 17.90 dBi, whereas the measured gain was 16.20 dBi. This gain is adequate for long-distance communications, and therefore, demonstrated the efficiency of proposed antenna and the feed in particular. To support this claim, the measured efficiency, which is the measured gain divided by the directivity was investigated as follows. The antenna solid angle Ω (which is the product of Ω_{xz} Ω_{yz} in *xz*- and *yz*-planes' HPBW) is approximately equals to 377.4°. The directivity of an ideal resonator then becomes 4π divided by the solid angle in radians, whereas, it is written in degree as $[4\pi \times (180/\pi)^2]/\Omega$. For a practical planar uniform array, the directivity D is given as D = 26,000/Ω,[31] which is equal to 68.89 for this design. The radiation efficiency (η), therefore, equals 41.69 ($10^{1.62}$ i.e. 16.2 dBi measured gain)/D = 0.67. The radiation efficiency is then calculated to be 60.7%. Thus the power radiated by the antenna is 60.7% of the total input power and it is concentrated along the

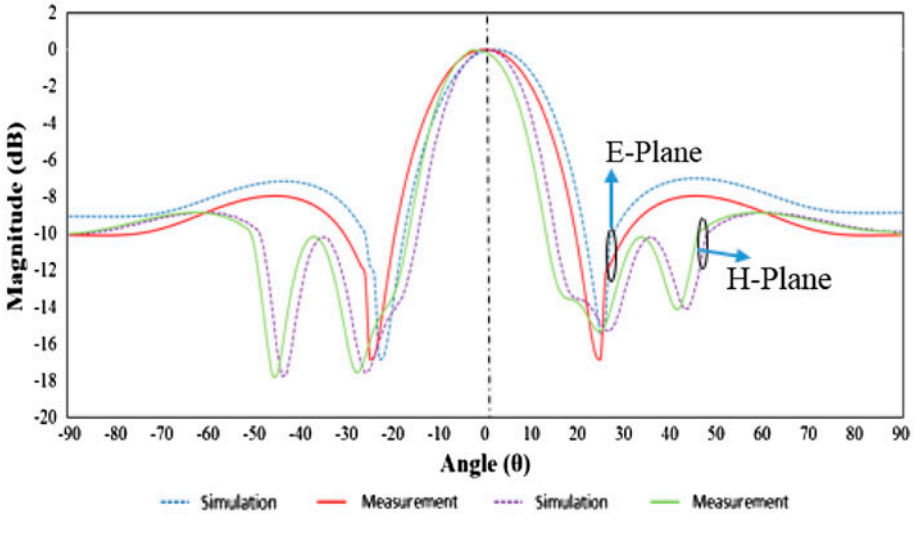

Figure 7. Normalized radiation pattern of the proposed antenna.

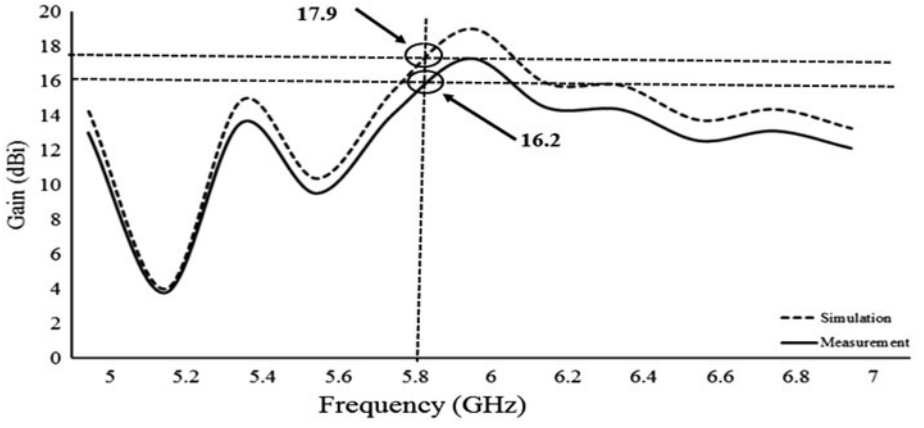

Figure 8. Simulated and measured gain of the proposed antenna.

principal axis of consideration. In Table 2, losses computation to assess the optimization was reported. The total systemic losses was 2.8662 dB, constituting about 4.97% systemic losses and indirectly 95.03% systemic efficiency. This was undoubtedly responsible for the significant gain of the proposed antenna.

The popular Q-factor equation ($Q = \omega W_T/P_T$) stated in [32] was used to calculate the systemic Q-factor, where ω is the angular frequency (at a frequency of 5.8 GHz) and W_T is the total energy stored by the radiator. The total power loss (P_T) calculated to be equal to 2.8622 as demonstrated in Table 2 can then be substituted in the Q-factor equation. Thereafter, the value of W_T was determined using equation stated in [33] and the value was in turn substituted into the Q-factor equation to determine its value which is equal to 0.66. Though the systemic Q-factor of about 0.7 as demonstrated in this work is adequate, it is however inferior to the inherent high Q-factor characteristics of the quasi-lumped element resonator antenna. One major cause of the reduction in Q-factor is the substrate loss which was not considered during the optimization except for dilectric loss. Usually, the substrate loss (particularly in practical substrate as against the ideal lossless substrate) occurs due to some energy coupled into the dielectric distance between the conducting planes of the substrate,[33] and the effect becomes more pronounced at higher ranges of frequency, once the frequency is higher than GHz. This effect essentially causes the resonator to radiates rather than store charges. Besides, the relative permitivity used is moderate. The 4.9% systemic losses in the antenna are responsible for the total losses in the proposed antenna. This total losses account for the radiation, conduction, dielectric and surface-wave losses. In all, the gain of the antenna is not affected by the polarization mismatch as well as the impedance mismatch otherwise known as the feed loss. The feed loss will of course account for the degree of mistmatch, and hence the return loss, VSWR and the bandwidth. However, the radiation effeciency is usually affected by conduction, dielectric inefficiencyand surface-wave incidences, resulting in their respective losses. To that effect, the increase in loss with sizes gives rise to a maximum gain value, and hence the 4.9% systemic losses can improve the antenna gain to the same degree. In general, a systemic losses of less than 5% is moderate and cannot degrade the systemic performance substantially.

5. Conclusion

An experimental study on the feasibility of implementing series array quasi-lumped element resonator antenna with corporate feed network, with appropriate feed optimization is presented. The simulation results closely agreed with experimental results. Though the corporate feed network has a disadvantage of wide antenna real estate, the size of the proposed antenna was moderately reduced at the instant of the compactness of the proposed resonator. Besides, the effects of feed network on high-gain antenna with complicated feed network were minimized by optimization procedure described earlier. To that effect, both gain, directivity and return loss were significant.

Acknowledgement

Authors wish to thank Universiti Sains Malaysia for grant No. 1001/PELET/854004RUT USM.

References

[1] Garg R, Bhartia P, Bahl I, Ittipiboon A. Microstrip antenna design handbook. 2nd ed. Boston (MA), London: Artech House Inc; 1998. p. 719–726.
[2] Zhu Q, Zhu J, Lu W, Wu L, Xu S. Dual-linearly polarized microstrip array based on composite right/left-handed transmission line. Microwave Opt. Technol. Lett. 2006;48:1366–1369.
[3] Petosa A. Dielectric resonator antenna handbook. Boston (MA), London: Artech House Inc.; 2007. p. 209–245.
[4] James JR, Hall PS, Wood C. Microstrip antenna theory and design. London: Peter Peregrinus; 1981.
[5] Pozar DM. Microstrip antennas. Proc. IEEE. 1992;80:79–81.
[6] Pozar DM, Shaubert DH. Scan blindness in infinite phased arrays on printed dipole. IEEE Trans. Antennas Propag. 1984;AP-32:602–610.
[7] Maulloux RJ. Phase array theory and technology. Proc. IEEE. 1982;70:246–291.
[8] Qian Y, Coccioli R, Sievenpiper D, Radisic V, Yablonovitch E, Itoh T. A microstrip patch antenna using a novel photonic band gap structures. Microwave J. 1999;42:66–76.
[9] Hong JS, Lancaster MJ. Microstrip filters for rf/microwave applications. New York (NY): Wiley; 2001.
[10] Bahl IJ. Lumped elements for RF and microwave circuits. Boston (MA), London: Artech House Inc.; 2003. p. 1–5.
[11] Bao XL, Ammann MJ. Comparison of several novel annular-ring microstrip patch antennas for circular polarization. J. Electromagn. Waves Appl. 2006;20:1427–1438.
[12] Yang R, Xie Y-J, Wang P, Li L. Microstrip antennas with left-handed materials substrates. J. Electromagn. Waves Appl. 2006;20:1221–1233.
[13] Tadjalli A, Sebak AR, Denidni TA. Resonance frequencies and far field patterns of elliptical dielectric resonator antenna: analytical approach. Prog. Electromagnet. Res. 2006;64:81–98.
[14] Kishk AA, Glisson AW, Junker GP. Bandwidth enhancement for split cylindrical dielectric resonator antennas. Prog. Electromagnet. Res. 2001;33:97–118.
[15] Song Y, Sebak AR. Radiation pattern of aperture coupled prolate hemispheroidal dielectric resonator antenna. Prog. Electromagnet. Res. 2006;58:115–133.
[16] Hwang SH, Moon JI, Kwak WI, Park SO. Printed compact dual band antenna for 2.4 and 5 GHz ISM band applications. IEE Electro. Lett. 2004;40:1568–1569.
[17] Ain MF, Olokede SS, Qasaymeh YM, Marzuki A, Mohammed JJ, Sreekantan S, Hutagalung SD, Ahmad ZA, Abdulla MZ. A novel 5.8 GHz quasi-lumped element resonator antenna. AEU - Int. J. Electr. Commun. 2013;67:557–563.
[18] WU K-L, Spenuk M, Litva J, Fang DG. Theoretical and experimental study of feed network effects on the radiation pattern of series-fed microstrip antenna arrays. Microwaves, Antennas Propag., IEE Proc. H. 1991;138:238–242.
[19] Levine E, Malamud G, Shtrikman S, Treves D. A study of microstrip array antennas with the feed network. Antennas Propag., IEEE Trans. 1989;37:426–434.

[20] Lewin L. Radiation from discontinuities in strip-line. Proceedings of the IEE – Part C: Monographs. 1960;107:163–170.
[21] Lewin L. Spurious radiation from microstrips. Proc. IEE. 1974;125:633–645.
[22] Perlmutter P, Shtrikman S, Treves D. Electric surface current model for the analysis of microstrip antennas with application to rectangular elements. Antennas Propag., IEEE Trans. 1985;33:301–311.
[23] Jayanthy T, Sugadev M, Ismaeel JM, Jegan G. Design and simulation of microstrip M-patch antenna with double layer. International Conference on Recent Advances in Microwave Theory and Applications, 2008. MICROWAVE 2008. 2008;230:21–24.
[24] Pucel RA, Masse DJ, Hartwig CP. Losses in microstrip. Microwave Theory Tech., IEEE Trans. 1968;16:342–350.
[25] Denlinger EJ. Losses of microstrip lines. Microwave Theory Tech., IEEE Trans. 1980;28:513–522.
[26] Wheeler HA. Transmission-line properties of parallel strips separated by a dielectric sheet. IEEE Trans. Microwave Theory Tech. 1965;MIT-13:172–185.
[27] Schneider MV. Microstrip lines for microwave integrated circuits. Bell Sys. Tech. J. 1969;48:1421–1455.
[28] Lee S, Hayakawa MA. study on the radiation loss from a bent transmission line. Electromagn. Compat., IEEE Trans. 2001;43:618–621.
[29] Ain MF, Qasaymeh YMA, Ahmad ZA, Zakariya MA, Othman MA, Sulaiman AA, Othman A, Hutagalung SD, Abdullah MZ. A novel 5.8 GHz high gain array dielectric resonator antenna. Prog. Electromagnet. Res. C. 2010;15:201–210.
[30] Ain MF, Lancaster MJ, Gardner P. Quasi-lumped element superconducting oscillator. TENCON 2004. 2004 IEEE Reg. 10 Conf. 2004;C,3:639–642.
[31] Johnson RC, Jasik H. Antenna engineering handbook. 2nd ed. New York (NY): McGraw-Hill Book Co.; 1984.
[32] Garg R, Bhartia P, Bahl I, Ittipiboon A. Microstrip antenna design handbook. Boston (MA): Artech House; 2001.
[33] Simovski CR, He S. Antennas based on modified metallic photonic bandgap structures consisting of capacitively loaded wires. Microwave Opt. Tech. Lett. 2001;31:1098–2760.